Supplementary Information

Materials and Methods

Fly stocks

The following fly stocks were kindly provided to us by our colleagues: *esg*^{ts}*>gfp* (Shigeo Hayashi), *Su(H)GBE-gal4* (Steven X Hou), *MyoIA*^{ts}*>gfp*, *UAS-Upd, esg*^{ts}*F/O* (Bruce Edgar) the double loss of function alleles *fz*^{H51}*,fz2*^{C1} (Jun Wu and Marek Mlodzik), *UAS-hep*^{wt}, *UAS-hep*^{act} (Aaron Diantonio), *dm*^{4} (Peter Gallant), *pygo*^{S123} (Mariann Bienz), *MARCM FRT2A* (Jean Paul Vincent), MARCM 82B (David Bilder). The rest of the lines used were obtained from VDRC and the Bloomington Stock collection.

RNAi lines: All lines used in this study belong to VDRC and have the corresponding ID numbers: *UAS-wg-IR* (13351) (Insertions in chrosmosomes II and III), *UAS-wg-IR* KK (104579), *UAS-wls-IR* KK (103812), *UAS-stat-IR* (43866), *UAS-myc-IR* (2947).

Genotypes

Figure 1

(A-A''') *UAS-dicer2/+*; *tub-gal80*^{ts}*/ +; how-gal4/+*

(B-B''', I) *UAS-dicer2/+*; *tub-gal80*^{ts}*/UAS-wg-IR; how-gal4/UAS-wg-IR*

(C, C') *UAS-dicer2/+; escargot-gal4, UAS-gfp/ tub-gal80*^{ts}*; how-gal4/UAS-wg-IR*

(D-F') *UAS-dicer2/+; escargot-gal4, UAS-gfp/+; tub-gal80*^{ts}*/+*

(G-H') *UAS-dicer2/+; escargot-gal4, UAS-gfp/UAS-wg-IR; tub-gal80*^{ts}*/UAS-wg-IR*

(J, K) *MyoIA-gal4/+; UAS-gfp, tub-gal80*^{ts}*/+*

(L) *MyoIA-gal4/UAS-wg-IR; UAS-gfp, tub-gal80*^{ts}*/UAS-wg-IR*

Figure 2

(Panels A-I):

UAS-dicer2/+; escargot-gal4, UAS-gfp/+; tub-gal80^{ts}/+

UAS-dicer2/+; escargot-gal4, UAS-gfp/UAS-wg-IR; tub-gal80^{ts}/ UAS-wg-IR

UAS-dicer2/+; escargot-gal4, UAS-gfp/UAS-wg-IR^{KK}; tub-gal80^{ts}/+

UAS-dicer2/+; escargot-gal4, UAS-gfp/UAS-wls-IR^{KK}; tub-gal80^{ts}/ +

(Panel J):

UAS-dicer2/+; tub-gal80^{ts}/ UAS-CD8-gfp; how-gal4/+

UAS-dicer2/+; tub-gal80^{ts}/UAS-wg-IR; how-gal4/UAS-wg-IR

UAS-dicer2/+; tub-gal80^{ts}/ UAS-wg-IR^{KK}; how-gal4/+

UAS-dicer2/+; tub-gal80^{ts}/ UAS-wls-IR^{KK}; how-gal4/+

(Panel K):

mef2-gal4/+; tub-gal80^{ts}/+

UAS-dicer2/+; mef2-gal4/; tub-gal80^{ts}; +/UAS-wg-IR

(Panel L):

yw; escargot-gal4, UAS-gfp/tub-gal80^{ts}; how-gal4/+

UAS-dicer2/+; escargot-gal4, UAS-gfp/ tub-gal80^{ts}; how-gal4/UAS-wg-IR

(Panel M):

y,w; escargot-gal4, UAS-gfp/Cyo; tub-gal80^{ts}/+

wg^{CX4}/Cyo

(Panel N):

MyoIA-gal4/+; UAS-gfp, tub-gal80^{ts}/+

MyoIA-gal4/UAS-wg-IR; UAS-gfp, tub-gal80^{ts}/UAS-wg-IR

MyoIA-gal4/UAS-wg-IR^{KK}; UAS-gfp, tub-gal80^{ts}/+

Figure 3

Panels (A-L, N-R):

w^{-}*; esg-gal4, tub-gal80*^{ts}*, UAS-gfp/+; UAS-flp, act>CD2>gal4/+*

w^{-}*; esg-gal4, tub-gal80*^{ts}*, UAS-gfp/UAS-wg-IR; UAS-flp, act>CD2>gal4/UAS-wg-IR*

w^{-}*; esg-gal4, tub-gal80*^{ts}*, UAS-gfp/UAS-wg-IR*^{KK}*; UAS-flp, act>CD2>gal4/+*

w^{-}*; esg-gal4, tub-gal80*^{ts}*, UAS-gfp/UAS-wls-IR*^{KK}*; UAS-flp, act>CD2>gal4/+*

(Panel M):

yw; escargot-gal4, UAS-gfp/+; tub-gal80^{ts}*/+*

UAS-dicer2/+; escargot-gal4, UAS-gfp/UAS-wg-IR; tub-gal80^{ts}*/UAS-wg-IR*

wg^{CX4}*/Cyo*

UAS-dicer2/+; *tub-gal80*^{ts}*/ UAS-CD8-gfp; how-gal4/+*

UAS-dicer2/+; *tub-gal80*^{ts}*/UAS-wg-IR; how-gal4/UAS-wg-IR*

Figure 4

(A, B, E) *yw, hs-flp,tub-gal4, UAS-gfp(nls)/+; tub-gal80 FRT2A/FRT2A*

(C, D, E) *yw, hs-flp,tub-gal4, UAS-gfp(nls)/+; tub-gal80 FRT2A/fz*^{H51}*, fz2*^{C1} *FRT2A*

(F, G, J) y*,w, hsFlp/+; UAS-CD8-gfp, tub-gal4/+; FRT82B, tub-gal80/Lac-Z, FRT82B*

(H, I, J) y*,w, hsFlp/+; UAS-CD8-gfp, tub-gal4/+; FRT82B, tub-gal80/pygo*^{S123}*, FRT82B*

(Panels K-Q):

w^{-}*; esg-gal4, tub-gal80*^{ts}*, UAS-gfp/+; UAS-flp, act>CD2>gal4/+*

w^{-}*; esg-gal4, tub-gal80*^{ts}*, UAS-gfp/+; UAS-flp, act>CD2>gal4/UAS-Tfc*^{DN}

(Panel R):

yw; escargot-gal4, UAS-gfp/+; tub-gal80^{ts}*/+*

yw; escargot-gal4, UAS-gfp/+; tub-gal80^{ts}*/UAS-Tcf*^{DN}

Figure 5

(A-C’) *yw; escargot-gal4, UAS-gfp/+; tub-gal80*^{ts}*/+*

(D) *yw; escargot-gal4, UAS-gfp/UAS-wg-IR; tub-gal80*^{ts}*/UAS-wgIR*

(Panels E-K):

w^{-}*; esg-gal4, tub-gal80*^{ts}*, UAS-gfp/+; UAS-flp, act>CD2>gal4/+*

w^{-}*; esg-gal4, tub-gal80*^{ts}*, UAS-gfp/UAS-myc-IR; UAS-flp, act>CD2>gal4/+*

(Panel L):

yw; escargot-gal4, UAS-gfp/+; tub-gal80^{ts}*/+*

dm^{4}*/+; escargot-gal4, UAS-gfp/+; tub-gal80*^{ts}*/+*

dm^{G0139}*/+; escargot-gal4, UAS-gfp/+; tub-gal80*^{ts}*/+*

(Panel M):

yw; escargot-gal4, UAS-gfp/+; tub-gal80^{ts}*/+*

yw; escargot-gal4, UAS-gfp/UAS-myc-IR; tub-gal80^{ts}*/+*

dm^{4}*/+; escargot-gal4, UAS-gfp/+; tub-gal80*^{ts}*/+*

dm^{G0139}*/+; escargot-gal4, UAS-gfp/+; tub-gal80*^{ts}*/+*

Figure 6

(A-D’, I) *Su(H)GBE-gal4, UAS-CD8-gfp/tub-gal80*^{ts} *; +/+*

(E-H’, I) *UAS-dicer2/+; Su(H)GBE-gal4, UAS-CD8-gfp/tub-gal80*^{ts} *; UAS-wg-IR/+*

(I) *Su(H)GBE-gal4, UAS-CD8-gfp/UAS-myc-IR, tub-gal80*^{ts} *; +/+*

Figure 7

(A, A’, E, F) *yw; escargot-gal4, UAS-gfp/+; tub-gal80*^{ts}*/+*

(B, B’, E) *yw; escargot-gal4, UAS-gfp/UAS-hep*^{act}*; tub-gal80*^{ts}*/+*

(C, C’) *yw; escargot-gal4, UAS-gfp/ UAS-hep*^{wt}*; tub-gal80*^{ts}*/+*

(D, D’) *MyoIA-gal4/ UAS-hep*^{wt}*; UAS-gfp, tub-gal80*^{ts}*/+*

(Panel G):

UAS-dicer2/+; escargot-gal4, UAS-gfp/UAS-hep^{wt}; tub-gal80^{ts}/+

UAS-dicer2/+; escargot-gal4, UAS-gfp/UAS-hep^{wt}; tub-gal80^{ts}/UAS-wgIR

UAS-dicer2/+; escargot-gal4, UAS-gfp/UAS-hep^{wt}; tub-gal80^{ts}/UAS-Tcf^{DN}

UAS-dicer2/+; escargot-gal4, UAS-gfp/+; tub-gal80^{ts}/UAS-wg-IR

UAS-dicer2/+; escargot-gal4, UAS-gfp/+; tub-gal80^{ts}/UAS-Ttcf^{DN}

Figure 8

(A, D', I, J) *yw; escargot-gal4, UAS-gfp/+; tub-gal80^{ts}/+*

(E, G, I, J) *UAS-dicer2/+; escargot-gal4, UAS-gfp/UAS-wg-IR; tub-gal80^{ts}/+*

(F, H, I, J) *dm^{4}/+; escargot-gal4, UAS-gfp/+; tub-gal80^{ts}/+*

(Panels I, J):

UAS-dicer2/+; tub-gal80^{ts}/UAS-wg-IR; how-gal4/+

wg^{CX4}/Cyo

dm^{G0139}/+; escargot-gal4, UAS-gfp/+; tub-gal80^{ts}/+

Figure S1

(Panel A):

UAS-dicer2/+; tub-gal80^{ts}/ +; how-gal4/+

UAS-dicer2/+; tub-gal80^{ts}/UAS-wg-IR; how-gal4/UAS-wg-IR

(Panels B-H'):

UAS-dicer2/+; escargot-gal4, UAS-gfp/+; tub-gal80^{ts}/+

UAS-dicer2/+; escargot-gal4, UAS-gfp/UAS-wg-IR; tub-gal80^{ts}/UAS-wg-IR

UAS-dicer2/+; escargot-gal4, UAS-gfp/UAS-wg-IR^{KK}; tub-gal80^{ts}/+

(I) *UAS-dicer2/+; tub-gal80^{ts}/UAS-wg-IR^{KK}; how-gal4/+*

(Panels J-N'):

MyoIA-gal4/+; UAS-gfp, tub-gal80^{ts}/+

MyoIA-gal4/UAS-wg-IR; UAS-gfp, tub-gal80^{ts}/UAS-wg-IR

<u>Figure S2</u>

(Panel A):

UAS-dicer2/+; escargot-gal4, UAS-gfp/+; tub-gal80^{ts}/+

UAS-dicer2/+; escargot-gal4, UAS-gfp/UAS-wg-IR; tub-gal80^{ts}/ UAS-wg-IR

UAS-dicer2/+; escargot-gal4, UAS-gfp/UAS-wg-IR^{KK}; tub-gal80^{ts}/+

UAS-dicer2/+; escargot-gal4, UAS-gfp/UAS-wls-IR^{KK}; tub-gal80^{ts}/ +

(Panel B):

UAS-dicer2/+; *tub-gal80^{ts}/ UAS-CD8-gfp; how-gal4/+*

UAS-dicer2/+; *tub-gal80^{ts}/UAS-wg-IR; how-gal4/UAS-wg-IR*

UAS-dicer2/+; *tub-gal80^{ts}/ UAS-wls-IR^{KK}; how-gal4/+*

(C, C') *mef2-gal4/+; tub-gal80^{ts}/+*

(D, D') *UAS-dicer2/+; mef2-gal4/ tub-gal80^{ts}; +/UAS-wg-IR*

(E, E') *UAS-dicer2/+; escargot-gal4, UAS-gfp/ tub-gal80^{ts}; how-gal4/+*

(F, F') *UAS-dicer2/+; escargot-gal4, UAS-gfp/ tub-gal80^{ts}; how-gal4/UAS-wg-IR*

(Panel G):

MyoIA-gal4/+; UAS-gfp, tub-gal80^{ts}/+

MyoIA-gal4/UAS-wg-IR; UAS-gfp, tub-gal80^{ts}/UAS-wg-IR

MyoIA-gal4/UAS-wg-IR^{KK}; UAS-gfp, tub-gal80^{ts}/+

<u>Figure S3</u>:

(A, B) *UAS-dicer2/+; escargot-gal4, UAS-gfp/+; tub-gal80^{ts}/+*

(C, D) *UAS-dicer2/+; escargot-gal4, UAS-gfp/UAS-wg-IR; tub-gal80^{ts}/ UAS-wg-IR*

(E, F) *wg^{CX4}/Cyo*

(G, H) *UAS-dicer2/+*; *tub-gal80*^{ts}*/ +; how-gal4/+*

(I, J) *UAS-dicer2/+*; *tub-gal80*^{ts}*/UAS-wg-IR; how-gal4/UAS-wg-IR*

(Panels K, Q):

yw; escargot-gal4, UAS-gfp/tub-gal80^{ts}*; how-gal4/+*

UAS-dicer2/+; escargot-gal4, UAS-gfp/ tub-gal80^{ts}*; how-gal4/UAS-wg-IR*

Figure S4

(A-D, M) *yw; escargot-gal4, UAS-gfp/+; tub-gal80*^{ts}*/ +*

(E-M) *yw; escargot-gal4, UAS-gfp/+; tub-gal80*^{ts}*/ UAS-Tcf*^{DN}

Figure S5

(A-E, J, K) *yw; escargot-gal4, UAS-gfp/+; tub-gal80*^{ts}*/+*

(F, G) *dm*^{4}*/+; escargot-gal4, UAS-gfp/+; tub-gal80*^{ts}*/+*

(C, H, I, L, M) *yw; escargot-gal4, UAS-gfp/ UAS-myc-IR; tub-gal80*^{ts}*/ +*

Figure S6

(A-C') *yw; escargot-gal4, UAS-gfp/+; tub-gal80*^{ts}*/+*

(D-E) *UAS-dicer2; escargot-gal4, UAS-gfp/UAS-hep*^{wt}*; tub-gal80*^{ts}*/+*

(F) *UAS-dicer2/+; escargot-gal4, UAS-gfp/UAS-hep*^{wt}*; tub-gal80*^{ts}*/UAS-wgIR*

(G) *UAS-dicer2/+; escargot-gal4, UAS-gfp/UAS-hep*^{wt}*; tub-gal80*^{ts}*/UAS-Tcf*^{DN}

(H) *UAS-dicer2/+; escargot-gal4, UAS-gfp/+; tub-gal80*^{ts}*/UAS-wg-IR*

(I) *UAS-dicer2/+; escargot-gal4, UAS-gfp/+; tub-gal80*^{ts}*/UAS-Ttcf*^{DN}

Figure S7

(A-B', E-H) *yw; escargot-gal4, UAS-gfp/+; tub-gal80*^{ts}*/+*

(C-D', E-H) *UAS-dicer2/+; escargot-gal4, UAS-gfp/UAS-wg-IR; tub-gal80*^{ts}*/UAS-wg-IR*

Figure S8

(A, A', F) *yw; escargot-gal4, UAS-gfp/UAS-Upd; tub-gal80*^{ts}*/+*

(B,B', F) *yw; escargot-gal4, UAS-gfp/+; tub-gal80*^{ts}*/+*

(C-E’) *yw; escargot-gal4, UAS-gfp/UAS-stat-IR; tub-gal80^{ts}/+*

(Panels G, H)

yw; escargot-gal4, UAS-gfp/+; tub-gal80^{ts}/+

UAS-Dicer2/+; escargot-gal4, UAS-gfp/UAS-wg-IR; tub-gal80^{ts}/UAS-wg-IR

yw; escargot-gal4, UAS-gfp/UAS-myc-IR; tub-gal80^{ts}/+

yw; escargot-gal4, UAS-gfp/+; tub-gal80^{ts}/UAS-Tcf^{DN}

Primer sequences

rpl32 f	AGGCCCAAGATCGTGAAGAA
rpl32 r	TGTTGCACCAGGAACTTCTTGAA
myc f	ATGCACATCACCGATCACAG
myc r	ATGGGCCATCTGGAACTGTA
wg f	CCAACCCCACGAAGTACAGA
wg r	CATGGATGGGGTGGTTTAAG
upd3 f	AGGCCATCAACCTGACCAAC
upd3 r	ACGCTTCTCCATCAGCTTGC
socs36e f	ATGACCGTGCACTCGCAAAT
socs36e r	CCTCGTAGCGGTCCATCTTG
	GGATCGGTGTTGAGTTGCTT

delta-f	
delta-r	TGTCTCATGTACGGCGGATA
puc-f	CATCTCGCCCAATCTGAACT
puc-r	CCCACAGAAGATGACGAAGG

Supplementary Figure Legends

Figure S1. Wg is upregulated in response to diverse damages in the adult *Drosophila* midgut (A-D) Quantitative real time PCR (RT-qPCR) for *wg* in whole midguts from the indicated genotypes. Note that VM knockdown of *wg* resulted in decreased total transcript levels in midguts (A), while knockdown in *ISCs/EBs* via *esg-gal4* had not effect (B). *wg* transcript levels increased upon intestinal damage (C), and knock down in ISCs/EBs prevented the upregulation (D). (E-N') Posterior midguts expressing *gfp* alone (E, E', G, G') or in combination with RNAi for *wg,* under *esg-gal4* (F, F', H, H'), *how-gal4* (I) or *MyoIA-gal4* (J-N') drivers treated with Suc, *Pe* or Bleomycin (Bleo), were stained with anti-Wg (red). Note that the expression of *wg-IR or wg-IR*^{KK} via *esg-gal4*, but not with *how-gal4* or *MyoIA-gal4*, suppressed the upregulation of Wg in response to damage. Scale bars: 40µm. Unless otherwise indicated midguts are oriented with posterior up.

Figure S2. Wg from the ISC/EB population but not the VM or ECs is required for ISC proliferation during regeneration. (A-B) Quantification of pH3^{+ve} cells in posterior midguts expressing *gfp*, or RNAi for *wg* or *wls* under the control of the *esg-gal4* (A) or *how-gal4* (B) drivers in response to treatments with Sucrose, DSS (left panels) or Bleomycin (right panels). (C-D') Tangential sections of control midguts (C, C') or midguts expressing *wg* RNAi (D, D') under the control of the muscle specific *mef2*-gal4 driver stained with Phalloidin (green) and anti-Wg antibody (red). Note the knockdown of Wg protein in muscle cells (arrows, compare D, D', with C, C'). Posterior is to the right. (E-F') Midguts overexpressing *gfp* only (E, E') or in combination with *wg* RNAi (F, F') under the control of combined *esg-gal4, UAS-gfp; how-gal4* (*esg; how*>*gfp*) drivers stained with anti-GFP (green) and anti-Wg (red). Note the knockdown of Wg protein in *escargot* expressing cells (arrows, compare F, F', with E, E'). Posterior is up. (G) Quantification of pH3^{+ve} cells in posterior midguts expressing RNAi for *wg* in ECs under the control of *MyoIA-gal4* in response to treatments with DSS (left), Bleomycin (middle) and *Pe* (right). Note that only midguts with *esg-gal4* driven wg or wls RNAi showed significant blockade in the regenerative response to damages. (*** p<0.0001 one-way ANOVA with Bonferroni's Multiple Comparison Test). Scale bars: 20μm

Figure S3. Wg is not essential for ISC maintenance. (A-J) posterior midguts from 7 and 30 day-old flies expressing control *gfp* only or together with RNAi interference for *wg* or heterozygous for the wg^{CX4} allele stained with anti-Delta (red). Note the increase in Delta^{+ve} cells in aged guts (compare A with B and G with H) and the suppression of this phenotype upon *wg* knock down or heterozygosity. (K, L) Midguts carrying combined (*esg; how>gfp*) drivers stained with anti-GFP. (M-P) Control (*esg; how>gfp)* midguts (M, N) or midguts with inducible combined *wg* knock down (*esg; how^{ts}>wg-IR)* aged and stained as in A-J. (Q) Quantification of Delta^{+ve} cells ISCs in posterior midguts as in M-P. Note that combined knock down of *wg* prevents the age-dependent increase in the number of ISCs but does not lead to significant change in ISC number in 30 versus 7 day old midguts. (*p=0.005 Student's t Test). Scale bars: 40μm

Figure S4. TCF is required for ISC proliferation in response to damage and long-term ISC maintenance in the adult *Drosophila* midgut. (A-H) Posterior midguts from flies expressing *gfp* alone or a dominant negative form of TCF (Tcf^{DN}) under the control of the *esg*-gal4 driver, treated with Suc (A, E), *Pe* (B, F), DSS (C, G) or Bleo (D, H). Note that in all conditions $esg^{ts}>Tcf^{DN}$ guts fail to proliferate. (I-L) $esg^{ts}>Tcf^{DN}$ midguts after 7 and 30 days of transgene overexpression. Anti-GFP (green) and Delta staining (red) indicates a loss of *esg*$^{+ve}$ cells after 30 days (compare K, K' with I, I' and L with J). (M) Quantification of pH3^{+ve} cells in posterior midguts as in A-H. (*** p<0.0001 one-way ANOVA with Bonferroni's Multiple Comparison Test). Note that expression of *Tcf*^{DN} all proliferation in response to damages. Scale bars: (A-H) 20µm; (I, I', K, K') 40µm; (J, L) 100µm.

Figure S5. *Myc* is required for ISC proliferation in response to damage and long-term ISC maintenance in the adult *Drosophila* midgut. (A-B') Posterior midguts expressing *gfp* alone or with RNAi for *dmyc* under the control of the *esg*-gal4 driver treated with Suc (A, A') or Bleo (B, B') and stained with anti-Myc (A, B; red and A', B'; grey). Note the upregulation of Myc upon damage. (C) Quantification of pH3^{+ve} cells in posterior midguts expressing *gfp* or RNAi interference for *dmyc* under the control of the *esg*-gal4 driver upon treatment with DSS and Bleo (*** p<0.0001 one-way ANOVA with Bonferroni's Multiple Comparison Test). Note that myc knock down completely suppressed proliferation in response to damage. (D-I) 7 and 30 day-old posterior midguts expressing *gfp* or RNAi interference for *myc* under the control of the *esg*-gal4 driver, or heterozygous for a loss of function allele of *dmyc* and stained with anti-Delta (red). Staining showed a suppression of the age-related ISC increase by *myc* heterozygotes (F, G) and loss of ISCs after 30 days of gene knock down in *esg*^{ts}*>myc-IR* midguts (H, I). The latter was confirmed by looking at *esg>gfp* progenitor cells (J-M). Arrow in I points to a single, Delta^{+ve} ISC as confirmed by its co-localization with *esg>gfp* (not shown). The rest of the signal did not correspond to cells of either the expected size or *esg>gfp*$^{+ve}$ (not shown) and therefore was interpreted as background. Note the age-dependent increase in *esg*$^{+ve}$ cells in 30 versus 7-day old control midguts. Scale bars: (A-B', D-I) 40µm; (J-M) 100µm.

Figure S6. Wg is downstream of JNK in response to damage in the intestine. (A-B) Wild type midguts treated with Sucrose (A) or DSS (B) stained with anti-pJNK (red). Note that pJNK is undetectable in unchallenged tissue, but present in ECs upon tissue damage with DSS (B'; arrows). (C-D') Midguts after 2-day expression of *gfp* alone or in combination with a constitutively active form of *hemipterous* (hep^{act}) under the *esg-gal4* driver, stained with anti-Myc (C, D; red and C', D'; grey). Note the increase in Myc levels in some esg^{ts}>hep^{act} cells (D, D'; arrows). (E-I) Midguts after 7-day expression of wild type *hep* (E), RNAi for wg (H) or Tcf^{DN} (I) alone or combination of the latter two with hep^{wt} (F and G), under *esg-gal4*. Note the suppression of *hep*-induced ISC proliferation by co-expression of Tcf^{DN} or RNAi for *wg*. Scale bars: 20µm

Figure S7. Wg is downstream of JNK in ageing *Drosophila* midguts

(A-D') 7 and 30 day-old midguts of the indicated genotypes stained with anti-pJNK (red) to assess JNK activation. Note that pJNK was upregulated in ECs and big nuclei esg^{+ve} cells in aged guts (B, B'; arrows). pJNK was still upregulated after 30 days of *wg* knockdown in progenitor cells by *esg-gal4* (D, D'; arrows; compare D' with B'), while the expansion of esg^{+ve} cells was suppressed. (E-H) RT-qPCR of whole midguts to assess *delta*, *puckered* (*puc*), *wg* and *myc* transcript levels in control and upon *wg* knockdown by *esg-gal4*, in young (7 days of adult life) and ageing (30 days of adult life) midguts. Note that all four transcripts were upregulated in aged guts (E and F). Levels of *puc* mRNA upregulation were not significantly different in aged controls versus esg^{ts}>*wg-IR* midguts (G), while *myc* transcript upregulation was attenuated upon *wg* knockdown (H). Scale bars: 20µm

Figure S8. Parallel activation of Jak/Stat and Wg/Myc during midgut regeneration. (A-E') Midguts of the indicated genotypes were stained with anti-Wg (A, A', E, E'), or anti-Myc (B-D') after treatment with Sucrose or DSS. Note that IL-6/Upd overexpression under *esg-gal4* (to activate JAK/STAT signalling) did not affect Wg levels (A, A'). Also, unlike controls (B), *marelle/stat92E* knockdowns failed to regenerate in response to DSS treatment (see lack up expansion of the *esg>gfp* reporter in D; compared with B, C), in spite of upregulation of Myc (D'; compare with B', C') and Wg (E'; compare with basal Wg levels such as in Figure S1E'). (F) RT-qPCR of whole midguts to assess transcript levels of *wg* in midguts after 6-day expression of *gfp* only or together with *upd* under *esg-gal4* showed lack of *wg* upregulation (F). (G, H) RT-qPCR for *upd3* (G) and *socs36e* (H) in midguts of the indicated genotypes after Sucrose or DSS feeding. Midguts subject to 14-day knocking down of *wg*, *myc* or *tcf* under *esg-gal4* maintained significant upregulation of JAK/Stat signaling in response to damage in spite of their failure to regenerate. A similar result was observed after *Pe* feeding (not shown). Scale bars: 40µm

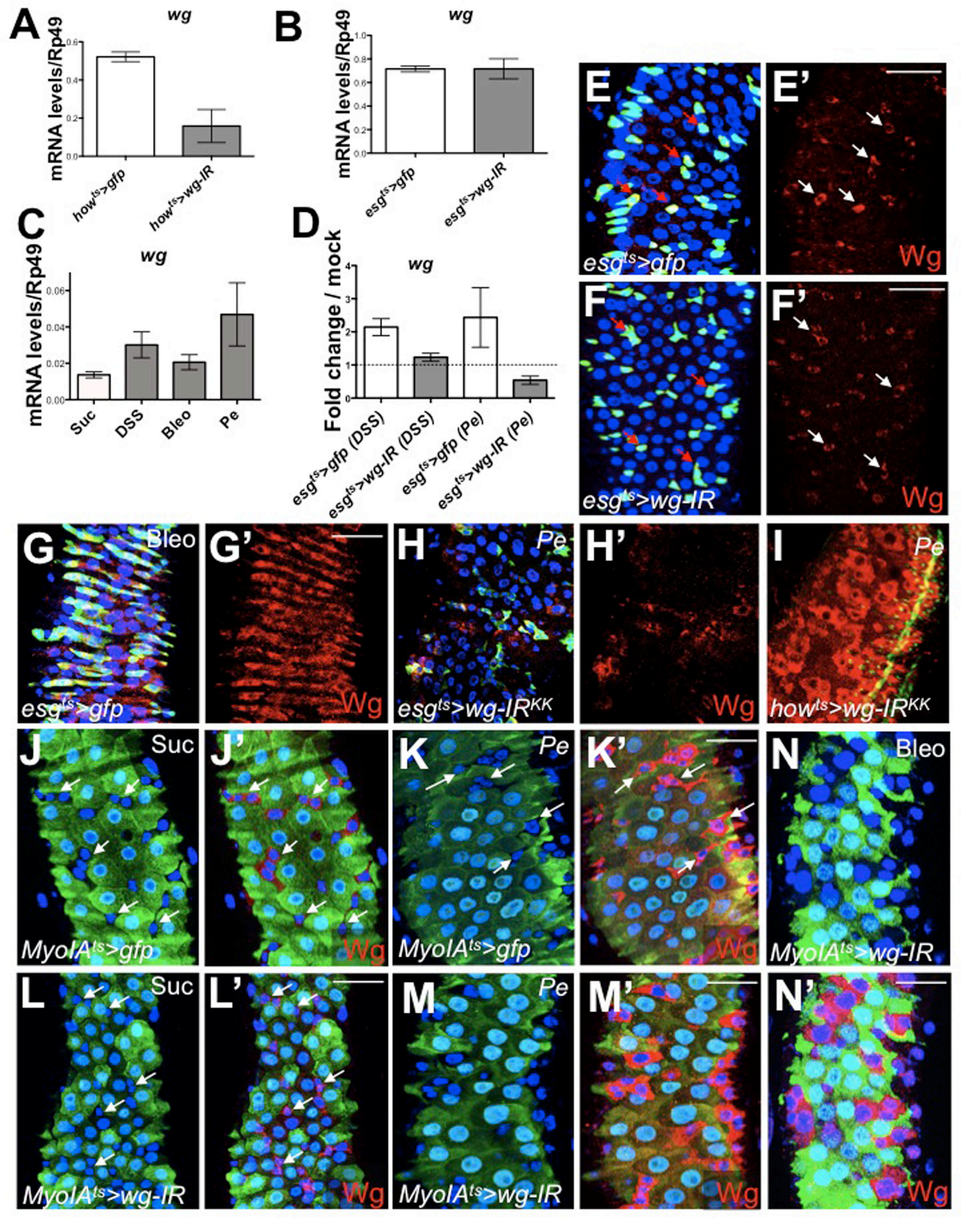

A
wg
mRNA levels/Rp49
how^ts>gfp
how^ts>wg-IR
B
wg
mRNA levels/Rp49
esg^ts>gfp
esg^ts>wg-IR
C
wg
mRNA levels/Rp49
Suc
DSS
Bleo
Pe
D
wg
Fold change / mock
esg^ts>gfp (DSS)
esg^ts>wg-IR (DSS)
esg^ts>gfp (Pe)
esg^ts>wg-IR (Pe)
E
E'
esg^ts>gfp
Wg
F
F'
esg^ts>wg-IR
Wg
G
Bleo
G'
esg^ts>gfp
Wg
H
Pe
H'
esg^ts>wg-IR^KK
Wg
I
Pe
how^ts>wg-IR^KK
J
Suc
J'
MyoIA^ts>gfp
Wg
K
Pe
K'
MyoIA^ts>gfp
Wg
N
Bleo
MyoIA^ts>wg-IR
L
Suc
L'
MyoIA^ts>wg-IR
Wg
M
Pe
M'
MyoIA^ts>wg-IR
Wg
N'
Wg

Figure S1

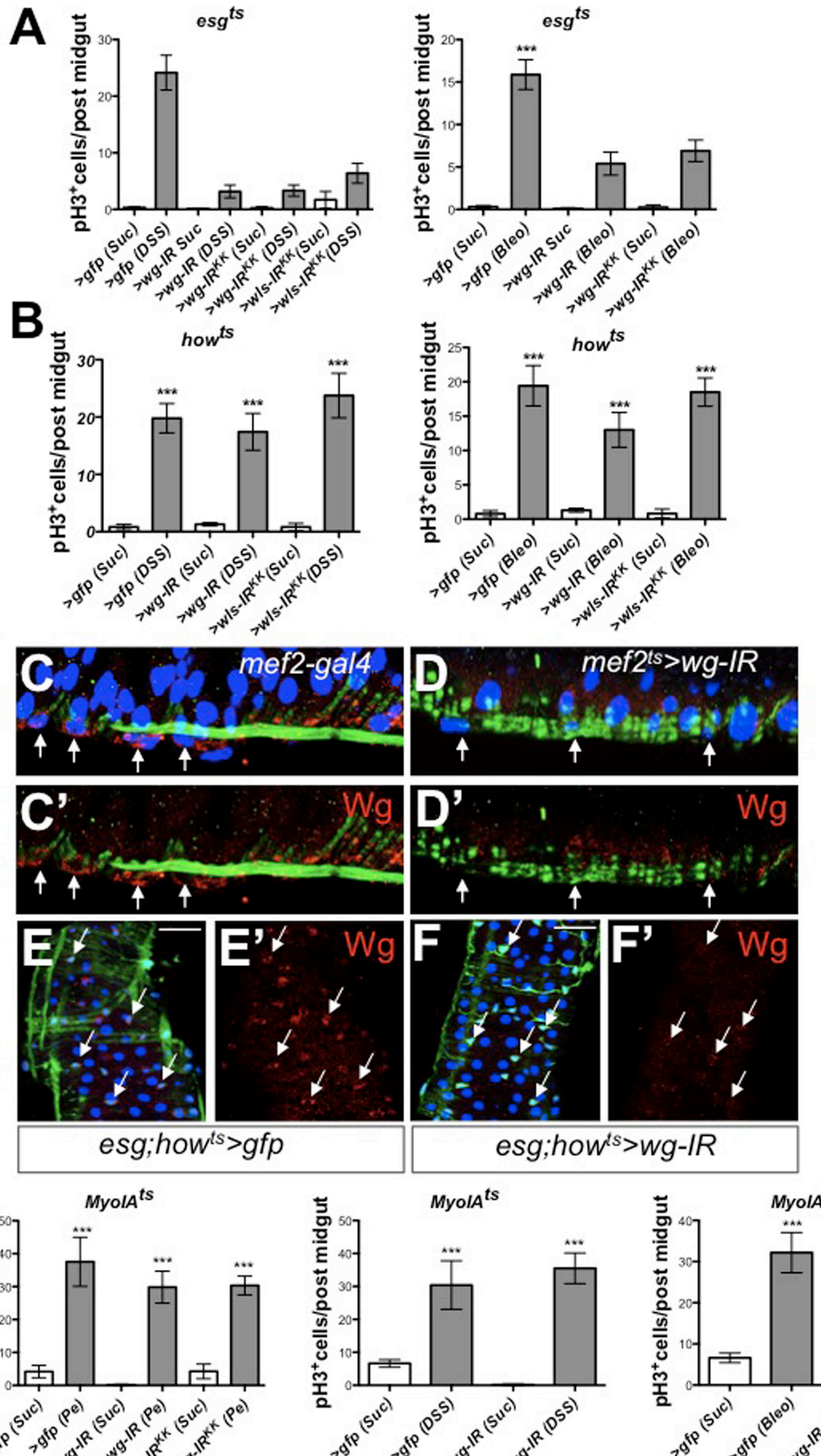
A
B
C
C'
D
D'
E
E'
F
F'
G
esgts
howts
mef2-gal4
mef2ts>wg-IR
Wg
esg;howts>gfp
esg;howts>wg-IR
MyoIAts
pH3+cells/post midgut

Figure S2

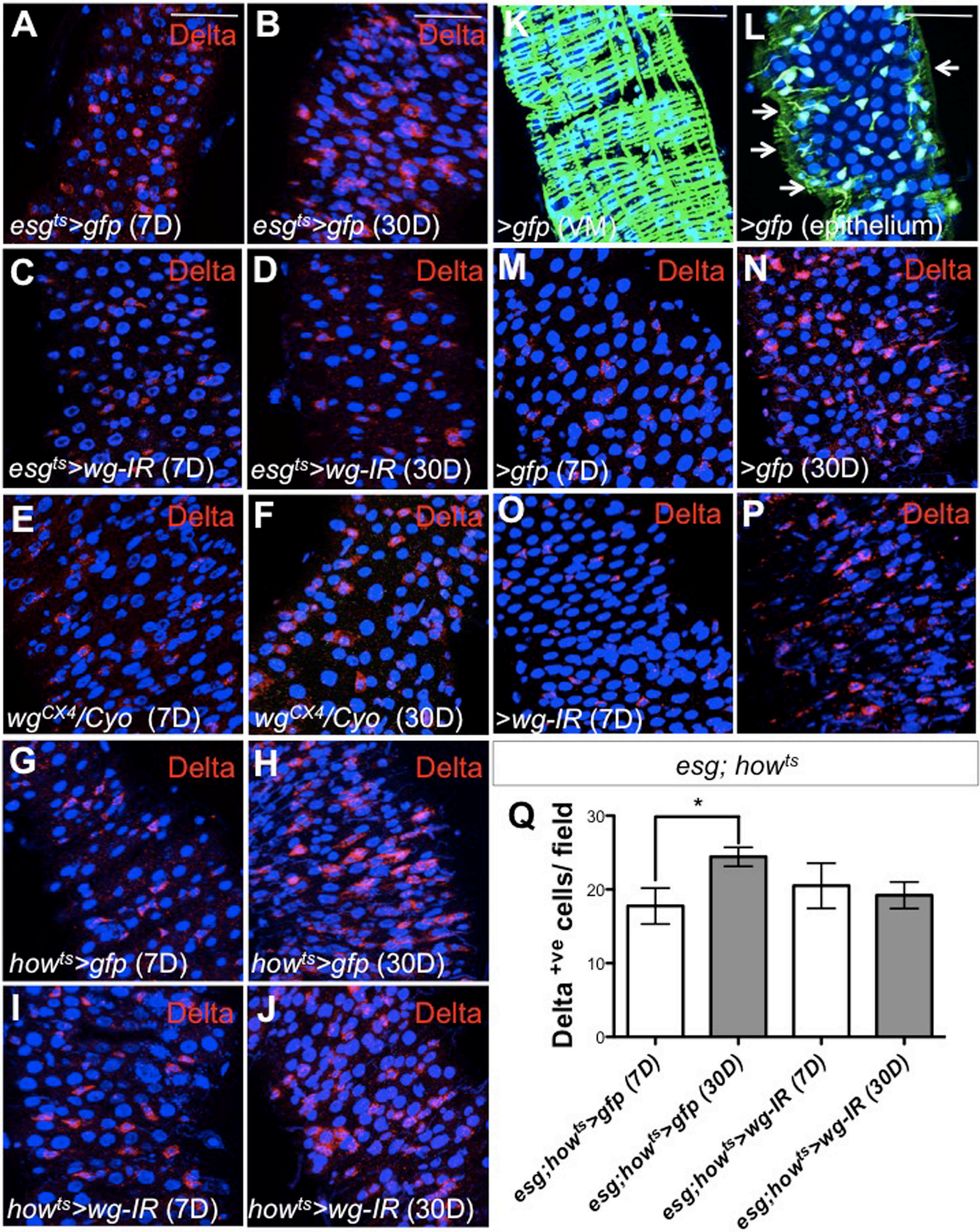
A
Delta
esgts>gfp (7D)
B
Delta
esgts>gfp (30D)
K
>gfp (VM)
L
>gfp (epithelium)
C
Delta
esgts>wg-IR (7D)
D
Delta
esgts>wg-IR (30D)
M
Delta
>gfp (7D)
N
Delta
>gfp (30D)
E
Delta
wgCX4/Cyo (7D)
F
Delta
wgCX4/Cyo (30D)
O
Delta
>wg-IR (7D)
P
Delta
G
Delta
howts>gfp (7D)
H
Delta
howts>gfp (30D)
I
Delta
howts>wg-IR (7D)
J
Delta
howts>wg-IR (30D)
esg; howts
Q
*
Delta +ve cells/ field
0
10
20
30
esg;howts>gfp (7D)
esg;howts>gfp (30D)
esg;howts>wg-IR (7D)
esg;howts>wg-IR (30D)

Figure S3

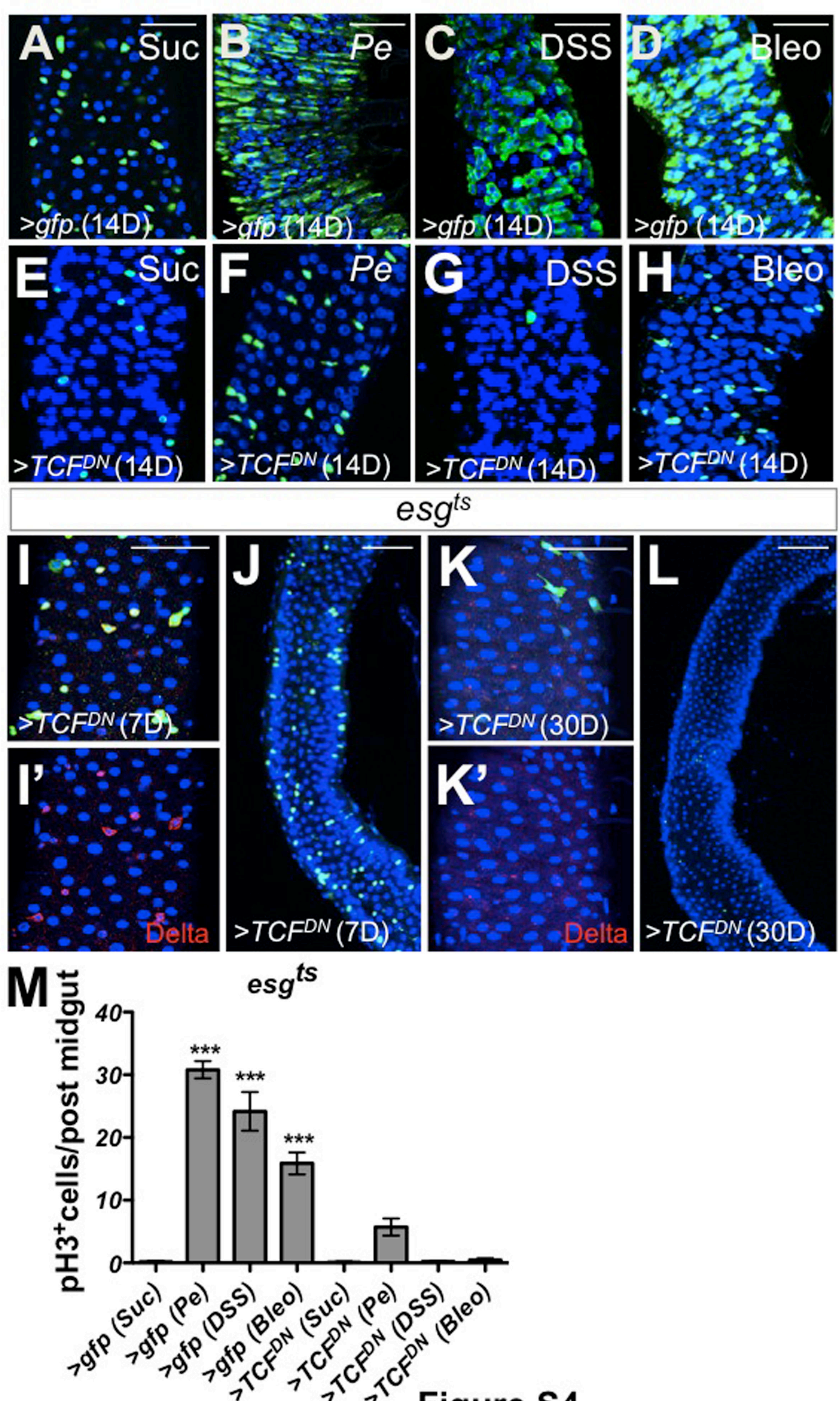

A Suc
B Pe
C DSS
D Bleo
>gfp (14D)
E Suc
F Pe
G DSS
H Bleo
>TCF^DN (14D)
esg^ts
I >TCF^DN (7D)
I' Delta
J >TCF^DN (7D)
K >TCF^DN (30D)
K' Delta
L >TCF^DN (30D)
M esg^ts
pH3+cells/post midgut
0
10
20
30
40
***
>gfp (Suc)
>gfp (Pe)
>gfp (DSS)
>gfp (Bleo)
>TCF^DN (Suc)
>TCF^DN (Pe)
>TCF^DN (DSS)
>TCF^DN (Bleo)

Figure S4

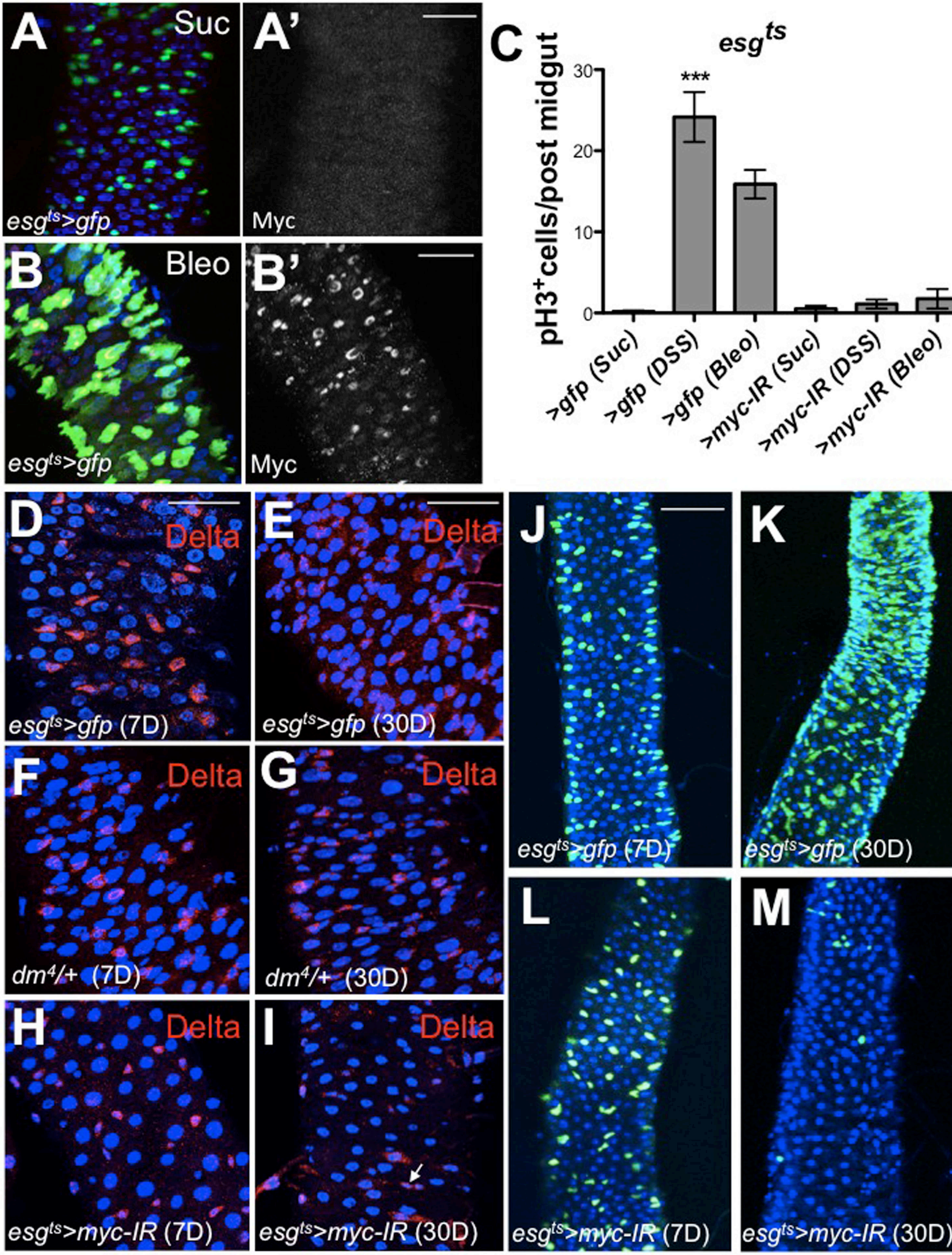

A
Suc
esgts>gfp
A'
Myc
B
Bleo
esgts>gfp
B'
Myc
C
esgts
pH3+cells/post midgut
***
>gfp (Suc)
>gfp (DSS)
>gfp (Bleo)
>myc-IR (Suc)
>myc-IR (DSS)
>myc-IR (Bleo)
D
Delta
esgts>gfp (7D)
E
Delta
esgts>gfp (30D)
F
Delta
dm4/+ (7D)
G
Delta
dm4/+ (30D)
H
Delta
esgts>myc-IR (7D)
I
Delta
esgts>myc-IR (30D)
J
esgts>gfp (7D)
K
esgts>gfp (30D)
L
esgts>myc-IR (7D)
M
esgts>myc-IR (30D)

Figure S5

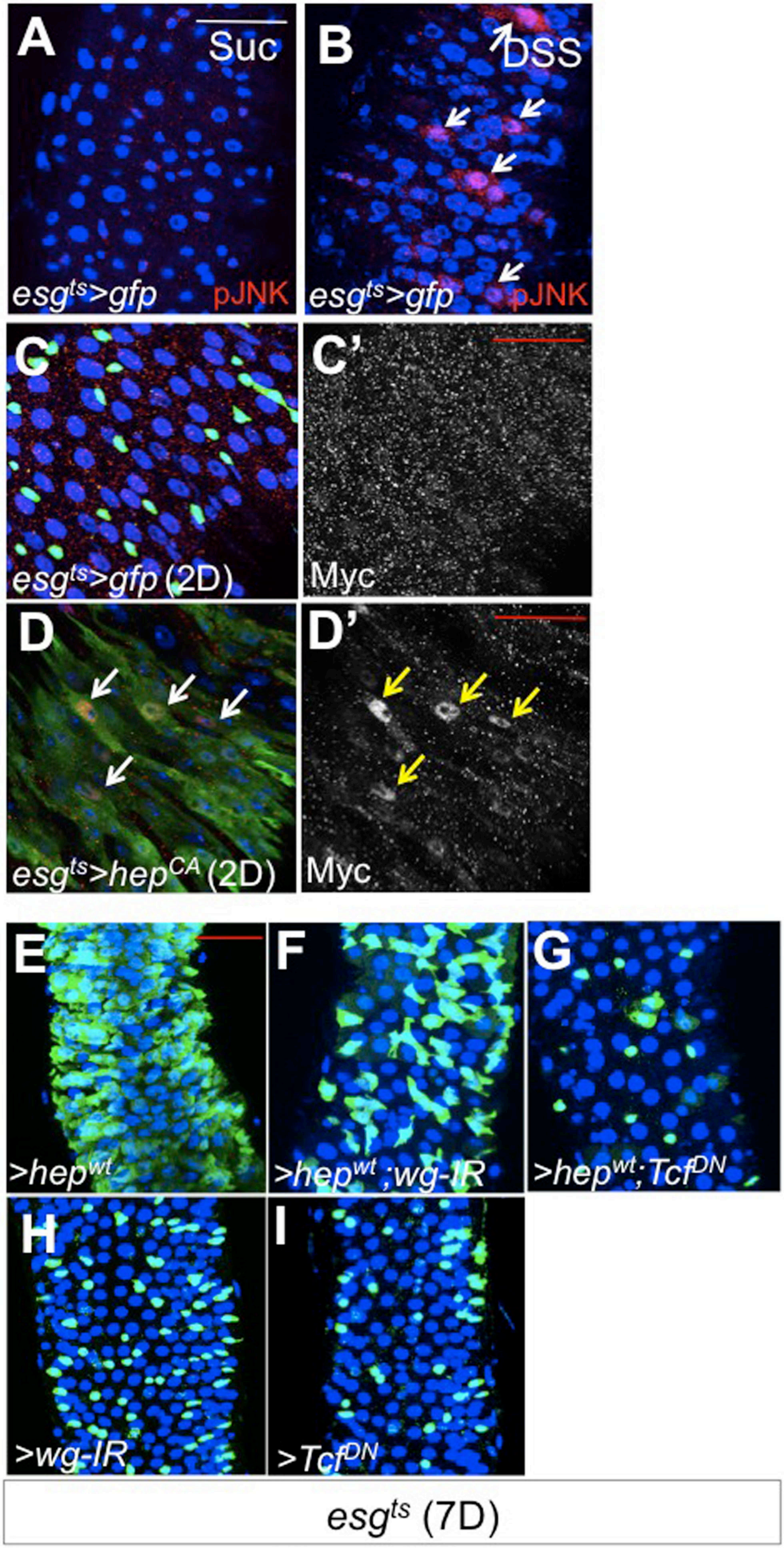

A
Suc
esgts>gfp
pJNK
B
DSS
esgts>gfp
pJNK
C
esgts>gfp (2D)
C'
Myc
D
esgts>hepCA (2D)
D'
Myc
E
>hepwt
F
>hepwt ;wg-IR
G
>hepwt;TcfDN
H
>wg-IR
I
>TcfDN
esgts (7D)

Figure S6

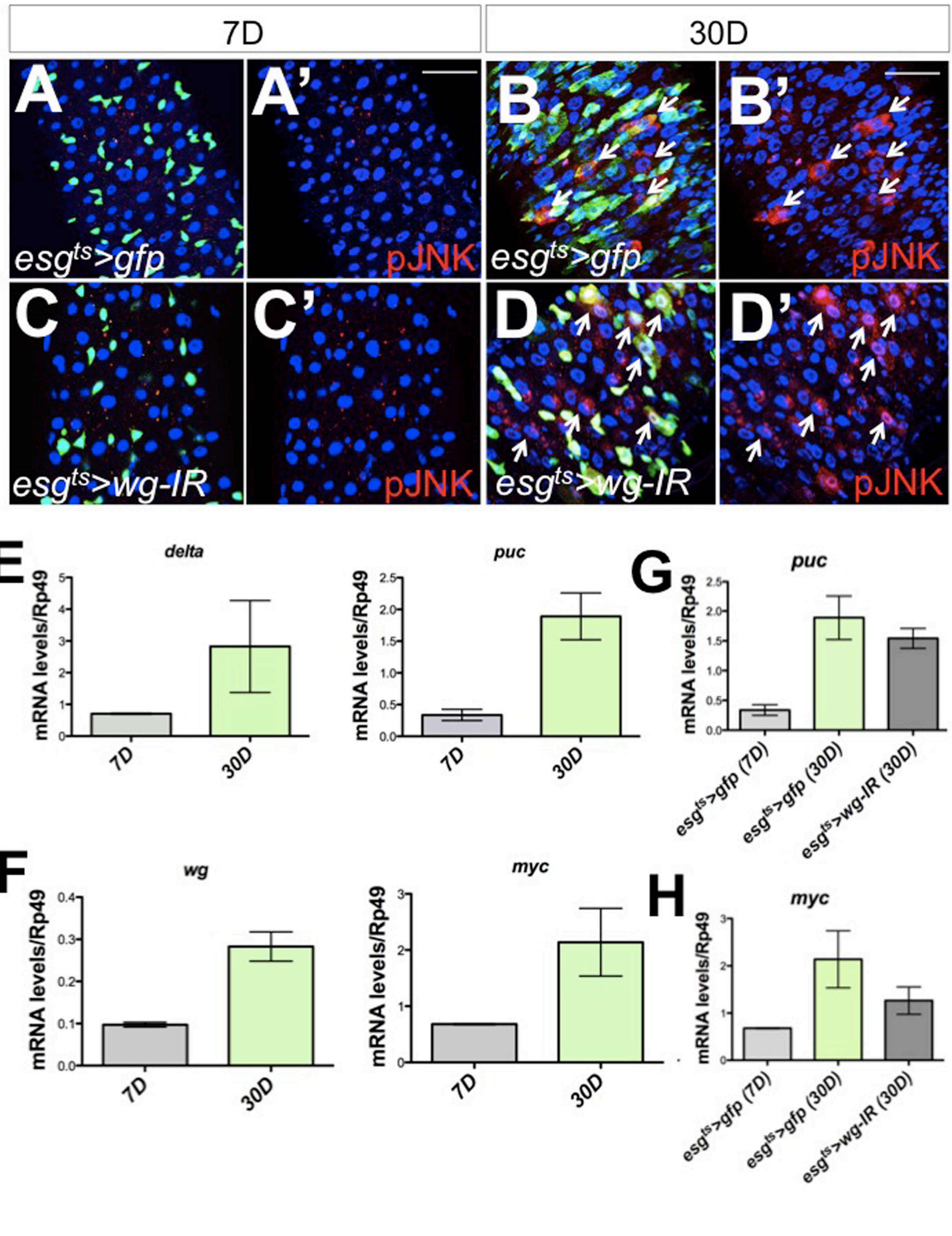
7D
30D
A
A'
B
B'
C
C'
D
D'
esgts>gfp
pJNK
esgts>gfp
pJNK
esgts>wg-IR
pJNK
esgts>wg-IR
pJNK
E
delta
mRNA levels/Rp49
7D
30D
puc
mRNA levels/Rp49
7D
30D
G
puc
mRNA levels/Rp49
esgts>gfp (7D)
esgts>gfp (30D)
esgts>wg-IR (30D)
F
wg
mRNA levels/Rp49
7D
30D
myc
mRNA levels/Rp49
7D
30D
H
myc
mRNA levels/Rp49
esgts>gfp (7D)
esgts>gfp (30D)
esgts>wg-IR (30D)

Figure S7

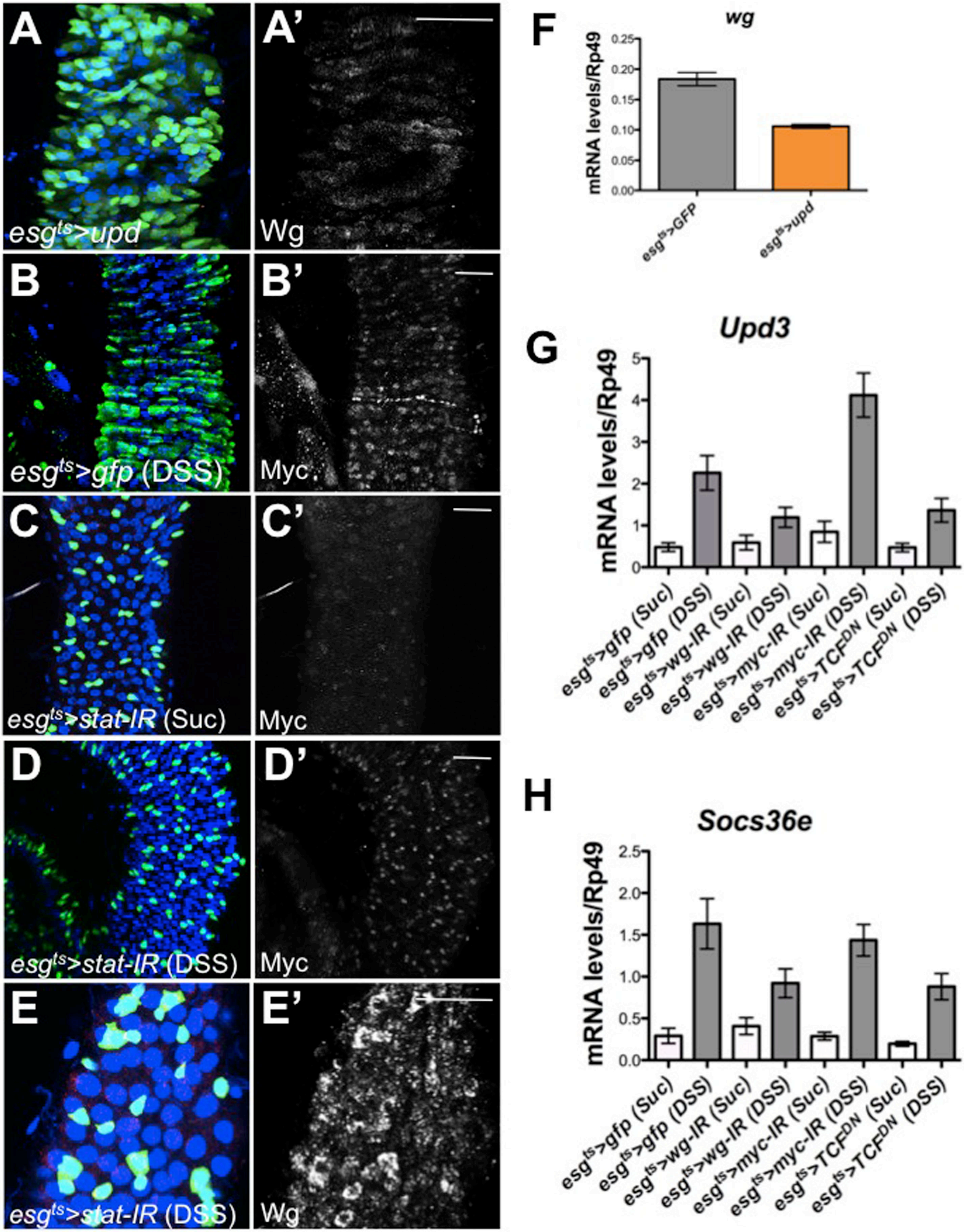

A
esg^ts>upd
A'
Wg
B
esg^ts>gfp (DSS)
B'
Myc
C
esg^ts>stat-IR (Suc)
C'
Myc
D
esg^ts>stat-IR (DSS)
D'
Myc
E
esg^ts>stat-IR (DSS)
E'
Wg
F
wg
mRNA levels/Rp49
0.25
0.20
0.15
0.10
0.05
0.00
esg^ts>GFP
esg^ts>upd
G
Upd3
mRNA levels/Rp49
5
4
3
2
1
0
esg^ts>gfp (Suc)
esg^ts>gfp (DSS)
esg^ts>wg-IR (Suc)
esg^ts>wg-IR (DSS)
esg^ts>myc-IR (Suc)
esg^ts>myc-IR (DSS)
esg^ts>TCF^DN (Suc)
esg^ts>TCF^DN (DSS)
H
Socs36e
mRNA levels/Rp49
2.5
2.0
1.5
1.0
0.5
0.0
esg^ts>gfp (Suc)
esg^ts>gfp (DSS)
esg^ts>wg-IR (Suc)
esg^ts>wg-IR (DSS)
esg^ts>myc-IR (Suc)
esg^ts>myc-IR (DSS)
esg^ts>TCF^DN (Suc)
esg^ts>TCF^DN (DSS)

Figure S8